Journal of Catalysis **183,** 107–118 (1999)
Article ID jcat.1998.2384, available online at http://www.idealibrary.com on IDEAL®

A Theoretical Study of the Solid Acid Catalyzed Desulfurization of Thiophene

Xavier Saintigny,* Rutger A. van Santen,* Sylvain Clémendot,† and François Hutschka†

*Schuit Institute of Catalysis, Laboratory of Inorganic Chemistry and Catalysis, Eindhoven University of Technology, P.O. Box 513, 5600 MB Eindhoven, The Netherlands; and †Total Raffinage Distribution, Centre Européen de Recherche et Technique, Département Chimie des Procédés, B.P. 27, 76700 Harfleur, France

Received September 22, 1998; revised December 9, 1998; accepted December 9, 1998

Desulfurization of thiophene upon contact with acidic zeolite has been studied theoretically using a DFT-based method. Two different mechanisms have been compared: one occurring in the absence of hydrogen and one occurring with the participation of hydrogen. Interestingly, the presence of hydrogen does not affect significantly activation barriers but dramatically changes the overall enthalpy of reaction. A detailed description of the two different mechanisms is given. © 1999 Academic Press

Key Words: **acid catalyst; DFT calculations; hydrodesulfurization; quantum chemistry; thiophene; transition states; zeolite.**

INTRODUCTION

Hydrotreatment, used extensively both for conversion of heavy feed stocks and for improving the quality of final products, represents one of the most important catalytic processes of the petroleum refining industry (1). Previously, hydrotreatment mainly consisted in the removal of hetero atoms such as sulfur, oxygen, and metals in order to protect the catalysts in downstream operations. Today, the greater needs for processing of heavier feeds, as both the supply of oil and the demand for fuel oil decline, have required more emphasis on hydrotreatment. Moreover, worldwide environmental legislation places increasingly severe restrictions on transportation fuels (2). Hence, processes such as deep desulfurization and dearomatization will become more important in order to provide environmentally more acceptable fuels.

Modern hydrocracking catalysts often consist of a combination of a sulfidic Ni–Mo or Ni–W phase and an acidic zeolite. Therefore, extensive studies have been performed on such metal sulfide catalysts in the last ten years (3, 4). Interestingly, it appears that removal of sulfur under catalytic cracking conditions can also occur. Such a reaction is catalyzed by the Brønsted acid sites of the zeolitic support. The activity of acidic zeolite in desulfurization has been experimentally demonstrated by several authors: López Agudo *et al.* have performed thiophene and DBT conversion studies using pure HZSM-5 zeolite (5), and Welters *et al.* have determined the HDS activities of pure CaY, USY, and H(46)NaY (4). The HDS tests of Welters *et al.* we refer to were performed at atmospheric pressure in a quartz tube.

These acid catalyzed reactions are not well understood. The theoretical study of desulfurization reaction paths of sulfur containing molecules upon contact with Brønsted acid sites will also provide a basis to a better understanding of the reactivity of such sites at the molecular level. Thiophene has been used as a model compound because it is the smallest sulfur containing an aromatic molecule.

First, a presentation of the method used will be given. It will be followed by a presentation of computed reaction energy diagrams for non-hydrogen activated and hydrogen activated reaction steps.

METHODS

To study reactions theoretically, reaction energy diagrams including the activation energies of the corresponding elementary steps have to be computed (6). The molecular system considered is a zeolitic cluster interacting with thiophene or reaction intermediates. The cluster $H_3SiOHAl(OH)_2OSiH_3$, named 3TOH for easier reference, has been used to represent the acidic zeolite. The current study is carried out with a "3T" fragment as it possesses two adjacent oxygens which retain the correct basicity (7). The main consequence of the use of clusters is the absence of any cavity-dependent effects (8). The cluster approach has well-known limitations (9), but on the other hand, due to finite computer resources and to the size of our systems, we have to do approximations. Our main interest is in qualitative trends that can help to explain experimental results. Elsewhere we discussed how this method can be complemented to include proper inclusion of microporous dependence (10). We have pointed out earlier that especially the concentration of adsorbed molecules sensitively depends on a match of

0021-9517/99 $30.00

molecular and micropore size. Since the interactions between the adsorbed molecule and micropores are dominated by van der Waals interactions, they cannot usually be included in the quantum chemical calculations. For small micropores one may expect that also the reaction energy diagrams may depend on the structure of a specific zeolite catalyst. Our results refer to the interaction energies due to the energetic changes of the reactive part of the molecule for the situations where pore size constraints are absent.

All calculations have been performed using the Becke-3-LYP hybrid method as implemented in Gaussian94 (11) and the basis set D95 (Dunning/Huzinaga full double-ζ (12)). We did not use any polarization functions for geometry optimization because of the size of our system and the computational cost of such calculations. However, single-point energy (SPE) corrections with the basis set D95**(D95 basis set and polarization functions on all atoms) were performed on all intermediaries and transition states.

Geometry optimization calculations have been carried out to a minimum for reactants, adsorption complexes, and products and to a saddle point for transition states (TS). The frequencies were computed using analytical second derivatives in order to check that the stationary point found exhibits the proper number of imaginary frequencies: none for a minimum and one for a transition state (first order saddle point).

Zero point energy (ZPE) corrections have been calculated for all optimized structures. All energies mentioned in the text below are ZPE-corrected unless otherwise stated. One has to point out that ZPE corrections do not include SPE corrections. The basis set superposition error was evaluated using the counterpoise method (7) and found negligible (the highest value is 2.4 kJ/mol).

No symmetry constraints have been used for any of the studied structures.

RESULTS AND DISCUSSION

Two different reaction pathways are possible in the HDS of thiophenic compounds: one with prehydrogenation of the heteroatom ring prior to C–S bond breaking and another one with direct S removal without previous saturation of the heteroatom ring (13).

In the current study, we focus on the second pathway, which corresponds to the direct sulfur removal. Two different mechanisms are considered. The first one will occur when no hydrogen is used and leads to the formation of butadiyne [1]. The other one will be observed when hydrogen is present which leads to the formation of butadiene [2].

$$\text{thiophene} \rightarrow \text{butadiyne} + H_2S \qquad [1]$$

$$\text{thiophene} + 2\ H_2 \rightarrow \text{(Z)-butadiene} + H_2S \qquad [2a]$$

$$\text{thiophene} + 2\ H_2 \rightarrow \text{(E)-butadiene} + H_2S \qquad [2b]$$

TABLE 1

Computed Thermodynamical Data and Rate Constant of Reactions [1], [2a], and [2b] (ΔrU, ΔrH and ΔrG in kJ/mol)

	ΔrU (0 K)	ΔrU (SPE)	ΔrU (ZPE)	ΔrH (298 K)	ΔrG (298 K)	k (s^{-1}) (298 K)
			D95			
[1]	341	361	302	313	261	1.6E−46
[2a]	−69	−59	−36	−44	−24	1.7E+04
[2b]	−84	−74	−51	−57	−40	9.0E+06
			D95**			
[1]	366		328	339	288	3.3E−51
[2a]	−54		−19	−25	−9	3.9E+01
[2b]	−69		−34	−40	−22	6.3E+03

The overall enthalpy and free energy for both reactions have been calculated using two different basis sets: D95 and D95** (Table 1). As one can see, energies found with both basis sets are consistent although the absolute difference is quite high (∼20 kJ/mol). However, one must point out that SPE corrections correct well the energies obtained from optimizations carried out with D95 basis set ($E_{SPE} - E_{D95**} =$ 5 kJ/mol). Table 1 shows that reaction [1] is too endothermic to occur. However, it is important to study the desulfurization mechanism in the absence of H_2 in order to determine the effect of H_2 on the activation barrier and on the structure of intermediates.

Mechanism of Desulfurization of Thiophene in the Absence of H_2

The mechanism of thiophene desulfurization in the absence of H_2 can be divided into two parts. The first part concerns the ring opening of thiophene and its subsequent deprotonation, leading to the formation of (1Z)but-1-ene-3-yne-1-thiol [*A*]. The second part of the mechanism deals with desulfurization of compound [*A*] with formation of butadiyne [*B*]. The molecules [*A*] and [*B*] adsorbed on the cluster give, respectively, the species **ths_two** and **sis**. Details of this mechanism are provided in Schemes 1 and 2.

In heterogeneous catalysis reactants have first to be adsorbed at the surface of the catalyst before reacting. Calculations show that thiophene can be adsorbed to the protonic cluster in two different modes having similar adsorption energies ($E_{ads} \sim -15$ kJ/mol). The first mode corresponds to the adsorption through the C–C bond (η^2 coordination mode) and the second one to the adsorption through the sulfur atom (η^1(S) coordination mode).

The computed adsorption values using clusters are far from the experimental values found in the literature for the absorption energies of aromatic molecules in medium pore zeolites ($E_{ads} \sim -60$ kJ/mol) (14). This is because cluster calculations do not account for the adsorption energy contribution provided by the micropores of the zeolite. Hence,

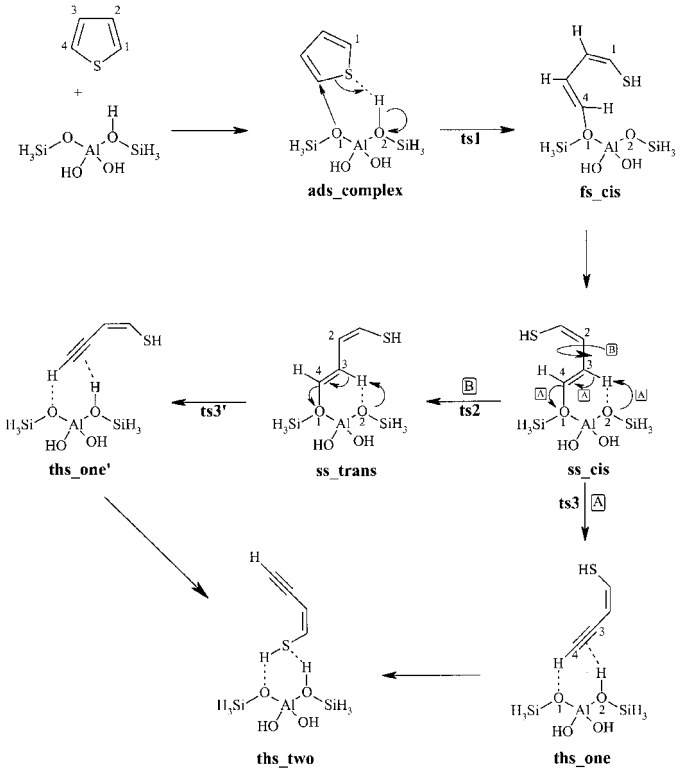

SCHEME 1. The first part of the desulfurization of thiophene by direct desulfurization in the absence of hydrogen reaction pathway mechanisms: opening of the thiophenic ring catalyzed by a pure acidic zeolite.

one has to add a "docking energy" to the adsorption energy calculated with the cluster method.

The adsorption mode η^1(S) is the only one leading to the protonation of the sulfur atom. The other adsorption mode, which leads to the aromatic ring hydrogenation, is out of the scope of the current study.

After adsorption of thiophene on the acidic site of the cluster, thiophenic ring opening occurs: the zeolitic hydrogen protonates the sulfur atom, the C4–S bond breaks, and a new bond between C4 and the zeolitic oxygen O1 is created (Scheme 1). The species **fs_cis** (first step: cis isomer compound) is obtained with the diene moiety in *cisoid* conformation as present in thiophene. The activation energy for this reaction is +222 kJ/mol (+279 kJ/mol with SPE correction) as one can see in Graph 1. The structure of transition state **ts1** is displayed in Graph 1. The high activation energy is due to the breaking of the strong C–S bond (13). Moreover, the species formed is much less thermodynamically stable than the reactants. Indeed the difference in energy between **ads_complex** and **fs_cis** is +109 kJ/mol (+119 kJ/mol with SPE correction). This loss of energy partially comes from the loss of aromaticity due to the ring opening. This assumption is confirmed by the value of the computed resonance energy (Er = +106 kJ/mol with no ZPE correction). A value which compares favorably with the experimental value found in the literature (Er_{exp} = +121 kJ/mol) (15).

In order to perform the next step, which corresponds to carbon C3 deprotonation, one needs to rotate the molecule through the O1–C4 bond. Such a rotation will create an interaction between proton H3 and oxygen O2 which is essential to back-donate proton H3 to the cluster. This rotation leads to the formation of compound **ss_cis**, which is slightly more stable than **fs_cis** because of the new interaction between H3 and O2. The determination of the transition state for this step is not of interest as this simple rotation through a single bond will have a very low activation barrier and hence will easily occur considering the experimental conditions.

At this point two different reaction pathways are possible. The compound **ss_cis** can back-donate proton H3 (Scheme 1, path A) or can swivel through the C2–C3 bond to form a more stable species **ss_trans** where the diene moiety is in *transoid* conformation (Scheme 1, path B). The activation barrier for the *cisoid–transoid* isomerization is +16 kJ/mol. The structure of transition state **ts2** is displayed in Fig. 1. Relatively low activation energy is obtained for this step and hence, this isomerization will easily occur.

In the next step, for both reaction paths proton H3 is back-donated to the zeolite and the bond between O1–C4 is broken. Both mechanisms lead to the same compound, **ths_one**, which is the adsorption complex through the triple bond of compound [*A*] on the zeolite. The only difference between **ths_one** and **ths_one**′ comes from the thiol group orientation in regards of the cluster (Scheme 1). This leads

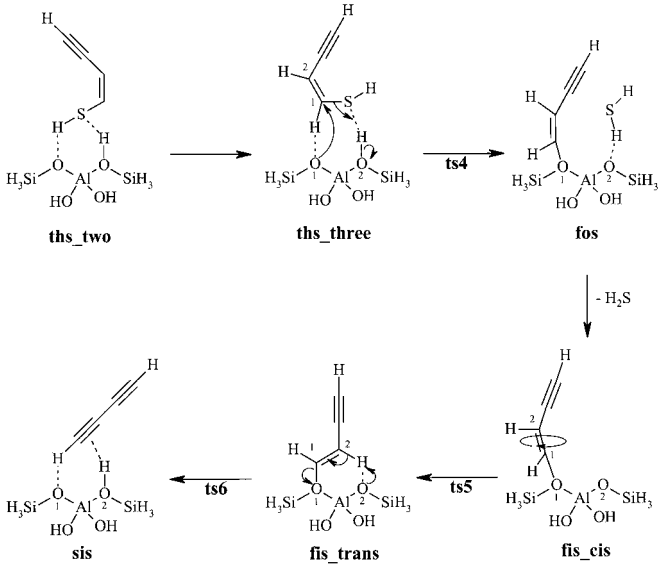

SCHEME 2. The second part of the desulfurization of thiophene by direct desulfurization in the absence of hydrogen reaction pathway mechanisms: removal of the sulfur atom of (1Z)but-1-ene-3-yne-1-thiol catalyzed by a pure acidic zeolite, leading to the formation of butadiyne.

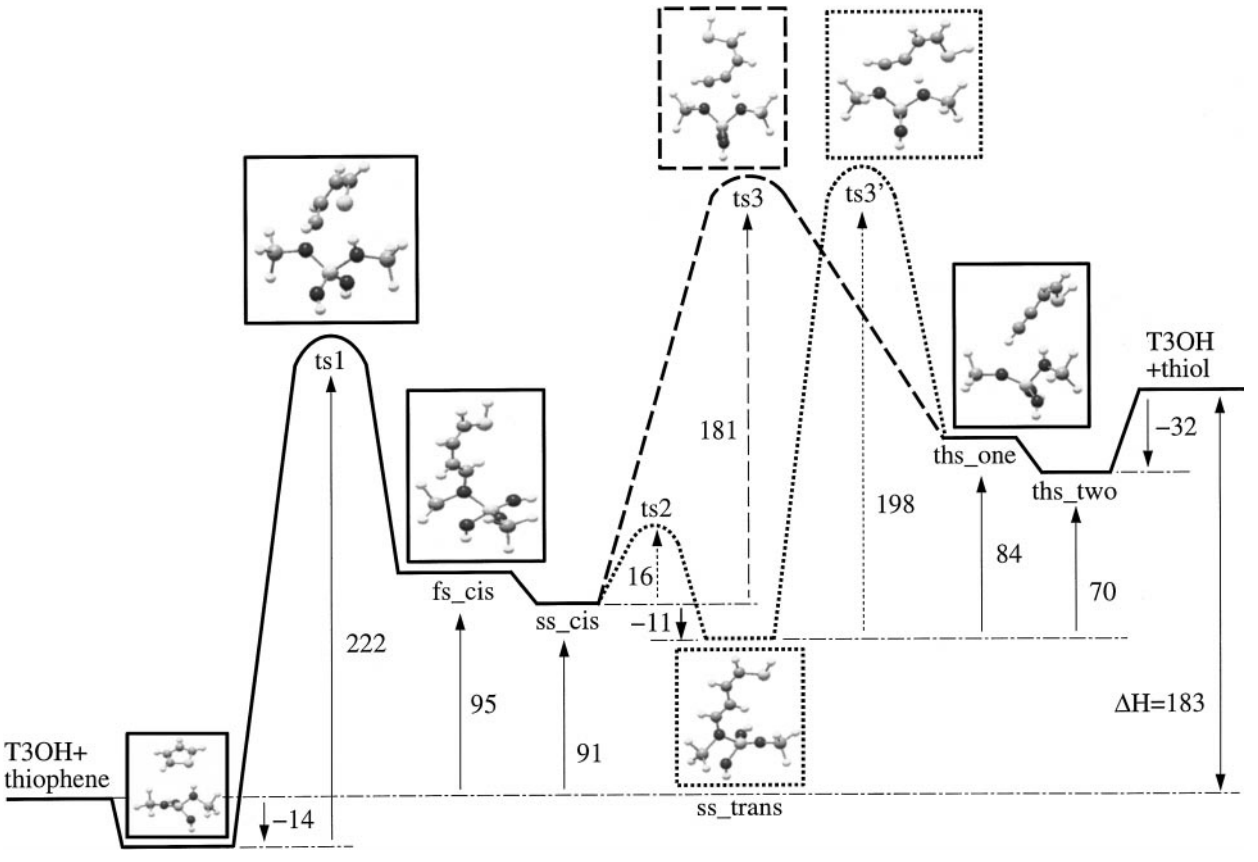

GRAPH 1. The reaction energy diagram and geometries of the transition states and intermediates for the first part of the direct desulfurization in the absence of hydrogen reaction path of thiophene catalyzed by a pure acidic zeolite. All the values are in kJ/mol.

only to a marginal energy modification, and then the two compounds energies are supposed to be similar. This step is also very endothermic ($\Delta E \sim 80$ kJ/mol) due to the formation of less favorable intermediates. In path A, the activation barrier for the back-donation of H3 is +181 kJ/mol (+208 kJ/mol with SPE correction). In path B, for this reaction step the activation barrier is +198 kJ/mol (+225 kJ/mol with SPE correction). The structures of transition states **ts3** and **ts3′** are very similar as one can see in Table 2 and Figs. 2 and 3. From these results, one can conclude that the reaction will proceed indiscriminately via path A or path B.

Then [*A*] may desorb from the zeolite and readsorb as structure **ths_two**, which is more stable. Compound [*A*] is then physically adsorbed (hydrogen-bonded) to the zeolite in an end-on position. The adsorption energy for this mode is −33 kJ/mol, which is two times higher than the one obtained for the adsorption of thiophene (η^1(S) coordination). This is because in **ads_complex** there is only the interaction between the sulfur atom and the zeolitic proton, whereas in **ths_two** two interactions are present: one between the S atom and the zeolitic proton and one between a zeolitic oxygen and the thiolic proton. Moreover, in **ths_two**, the sulfur electrons are not involved in an aromatic ring. Note that the computed adsorption energy for the end-on adsorption complex of methanethiol on the zeolite is $E_{ads} = -28$ kJ/mol. Furthermore, the adsorption energy calculated for the end-on adsorption complex of

TABLE 2

Geometries of the Transition States ts3 and ts3′ (bonds in angstrøm, angles in degree)

	ts3	ts3′
H4–C4	1.072	1.074
C4–C3	1.276	1.274
C4–O1	2.036	1.961
C3–C2	1.457	1.456
C3–H3	1.463	1.583
H3–O2	1.139	1.084
Si1–O1–Al	131.5	130.1
O1–Al–O2	96.2	95.6
Al–O2–Si2	130.0	130.7
C4–O1–Al	114.2	115.0
C3–C4–H4	160.2	155.4
O2–H3–C3	168.5	164.3
C4–C3–H3–O2	27.3	14.4
O1–C4–C3–H3	3.4	2.9
Al–O2–H3–C3	−9.1	6.4

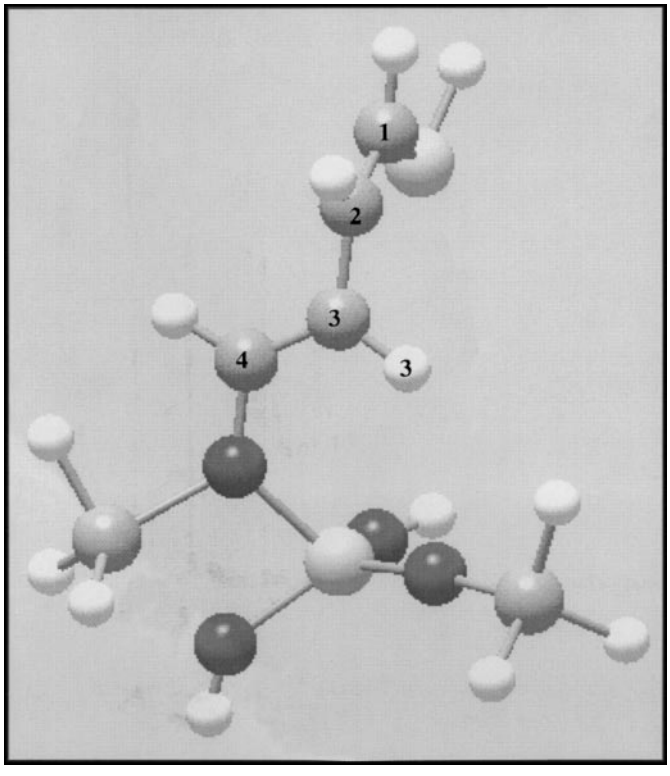

FIG. 1. Structure of the transition state **ts2**.

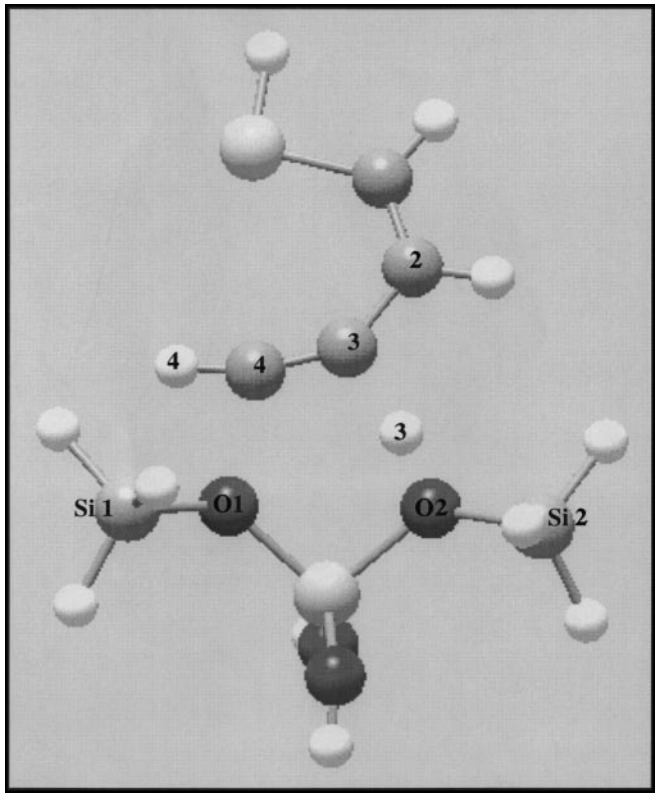

FIG. 2. Structure of the transition state **ts3**.

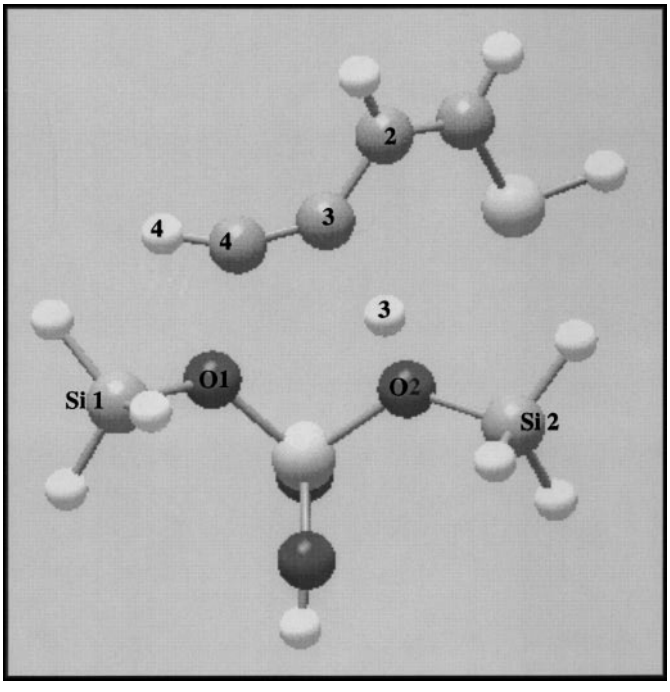

FIG. 3. Structure of the transition state **ts3′**.

methanol on the zeolite is −81 kJ/mol, which is 2.5 times higher than the one found for methanethiol.

From these results one can conclude that the low adsorption energies found when the sulfur atom is involved are due to weak hydrogen bonds between the zeolite and molecules because of the low electronegativity of sulfur compared to oxygen.

The second part of the mechanism corresponds to the desulfurization of compound [*A*]. The reaction proceeds via protonation of the S atom (as in the case of thiophene) which leads in several steps to compound [*B*] (Scheme 2).

Another adsorption mode for [*A*] was optimized in which the compound is adsorbed in a side-on position (**ths_three**). The adsorption energy for this mode is also quite low ($E_{ads} = -21$ kJ/mol) and consistent with values found for the two other modes. When [*A*] is adsorbed in the end-on position, the carbon–sulfur bond breaking cannot occur as carbon C1 is too far from any basic site of the cluster. Once adsorbed in the side-on position, the C–S bond breaking can occur while the zeolitic hydrogen H2 protonates the sulfur atom and a new bond, between O1 and C1, is created. Hence, a molecule of H_2S is formed along with another species covalently bonded to the cluster. The activation barrier is 183 kJ/mol, 39 kJ/mol lower than the one calculated for the thiophenic ring opening which also involved a C–S bond breaking. Such a difference is related to the fact that in thiols C–S bonds are weaker than in thiophene (16).

Then, H_2S desorbs from the cluster leading to structure **fis_cis**. The loss of energy for this step is 7 kJ/mol as H_2S was weakly adsorbed on the cluster.

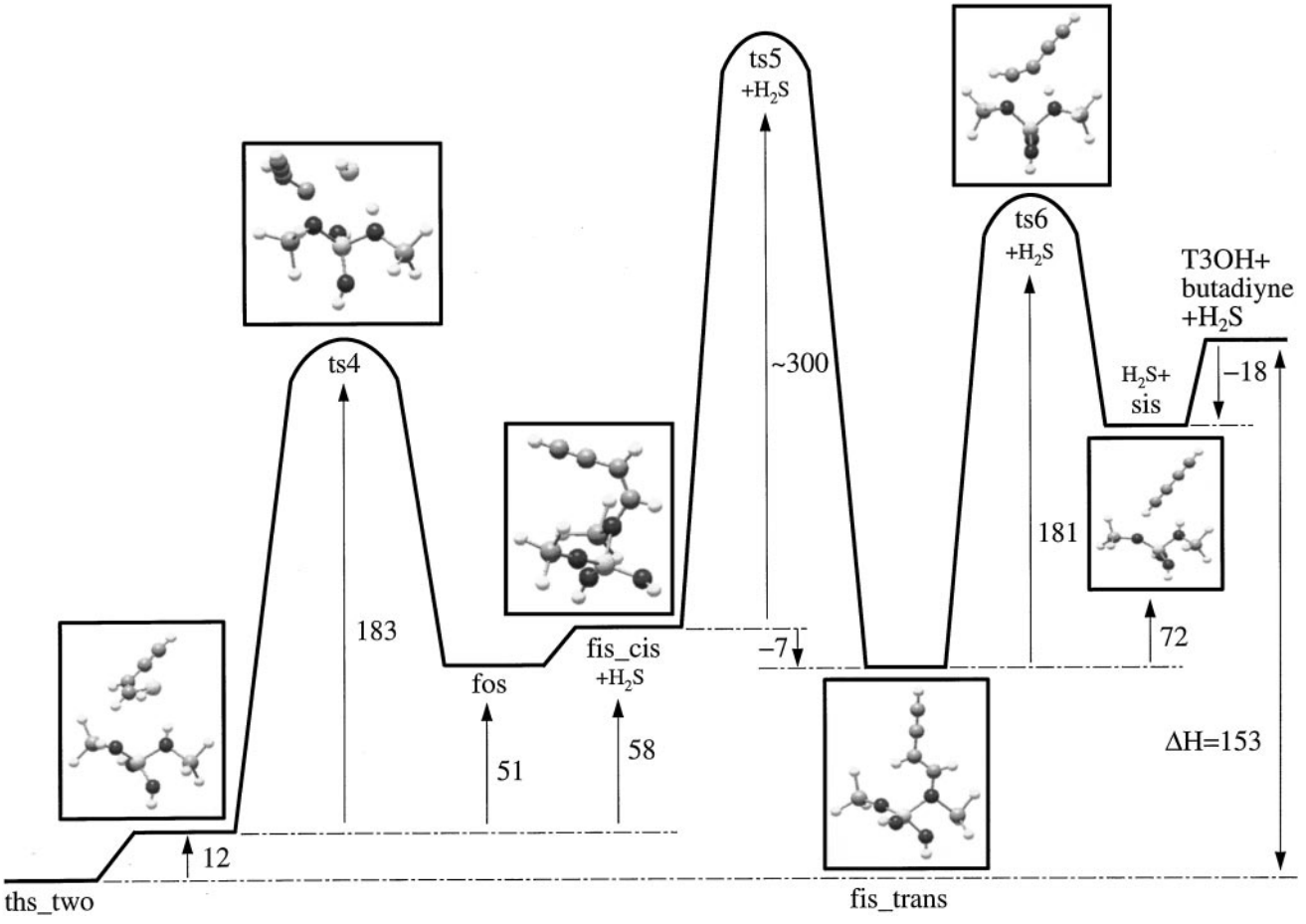

GRAPH 2. The reaction energy diagram and geometries of the transition states and intermediates for the second part of the direct desulfurization reaction in the absence of hydrogen path of thiophene catalyzed by a pure acidic zeolite. All the values are in kJ/mol.

The next step of the mechanism corresponds to the deprotonation of carbon C2. This cannot be achieved with structure **fis_cis** as hydrogen H2 is too far from any basic site of the cluster. To perform this step, one needs to isomerize the double bond present in compound **fis_cis** from the *cis* to the *trans* configuration. Compound **fis_trans** is obtained and it is more stable than **fis_cis** as one can expect (Graph 2). The transition state for this step has been determined using a smaller system to reduce the computational time required. Compound (1Z)but-1-ene-3-yne-1-ol (Fig. 4) has been used as a **fis_cis** analog as the geometry and Mulliken charges of both compounds are very similar (Table 3). Hence, such a system should give an estimation of the activation barrier for the *cis–trans* isomerization of compound **fis_cis**. The calculated activation energy is 300 kJ/mol, which compares well with the typical experimental value found for simple alkenes (260–270 kJ/mol) (17).

Once **fis_trans** is formed, proton H2 can be back-donated to the cluster to form structure **sis** where [*B*] is adsorbed on the cluster via one of the triple bonds. This step is analogous to the one leading to **ths_one** in the first part of the

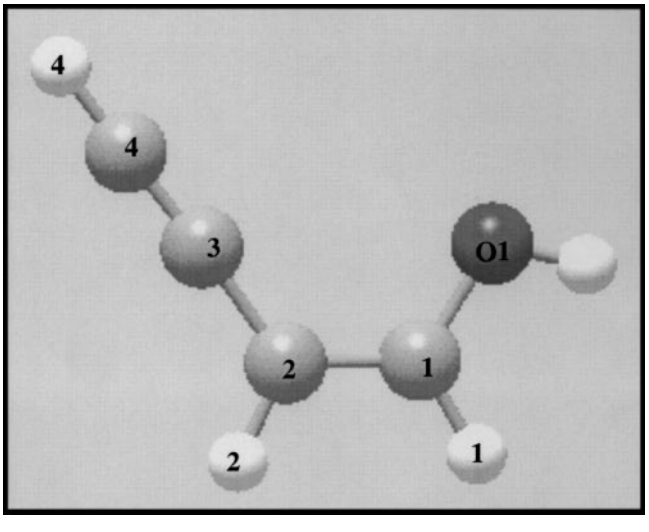

FIG. 4. Structure of (1Z)but-1-ene-3-yne-1-ol.

TABLE 3

Geometries and Mulliken Charges of the Species fis_cis and fis_cis analog

	fis_cis	fis_cis analog
O1–C1	1.405	1.391
C1–C2	1.352	1.356
C1–H1	1.087	1.091
C2–C3	1.430	1.429
C2–H2	1.089	1.088
C3–C4	1.225	1.227
C4–H4	1.067	1.066
O1–C1–C2	123.6	122.1
C1–C2–C3	125.9	125.6
C1	0.012	−0.092
H1	0.259	0.201
C2	−0.241	−0.285
H2	0.226	0.224
C3	0.176	0.183
C4	−0.430	−0.446
H4	0.280	0.272

mechanism. Similar activation barriers were found (198 kJ/mol for **ss_trans** and 181 kJ/mol for **fis_trans**) and geometries of both transition states are nearly the same (Graphs 1 and 2). The adsorption energy of [*B*] is −18 kJ/mol, which is close to the value found for **ths_one** (−19 kJ/mol) where compound [*A*] is adsorbed in the same mode.

The main characteristics of this mechanism are high activation barriers and a high overall enthalpy of reaction. The limiting step for this reaction is the *cis–trans* isomerization of compound **fis_cis**. The second limiting step of the mechanism is the thiophenic ring opening. The reaction is highly exothermic (−302 kJ/mol) and activation energies are around 200 kJ/mol (except for the *cis–trans* isomerization) (Graph 3).

When no hydrogen is present, desulfurization of thiophene with pure acidic zeolite is not possible. However, results show that the reverse reaction, which is thiophene formation from butadiyne and H_2S, can occur under acid catalytic conditions. Thus, the present mechanisms enable, at least, a better understanding of the energies of the corresponding elementary steps.

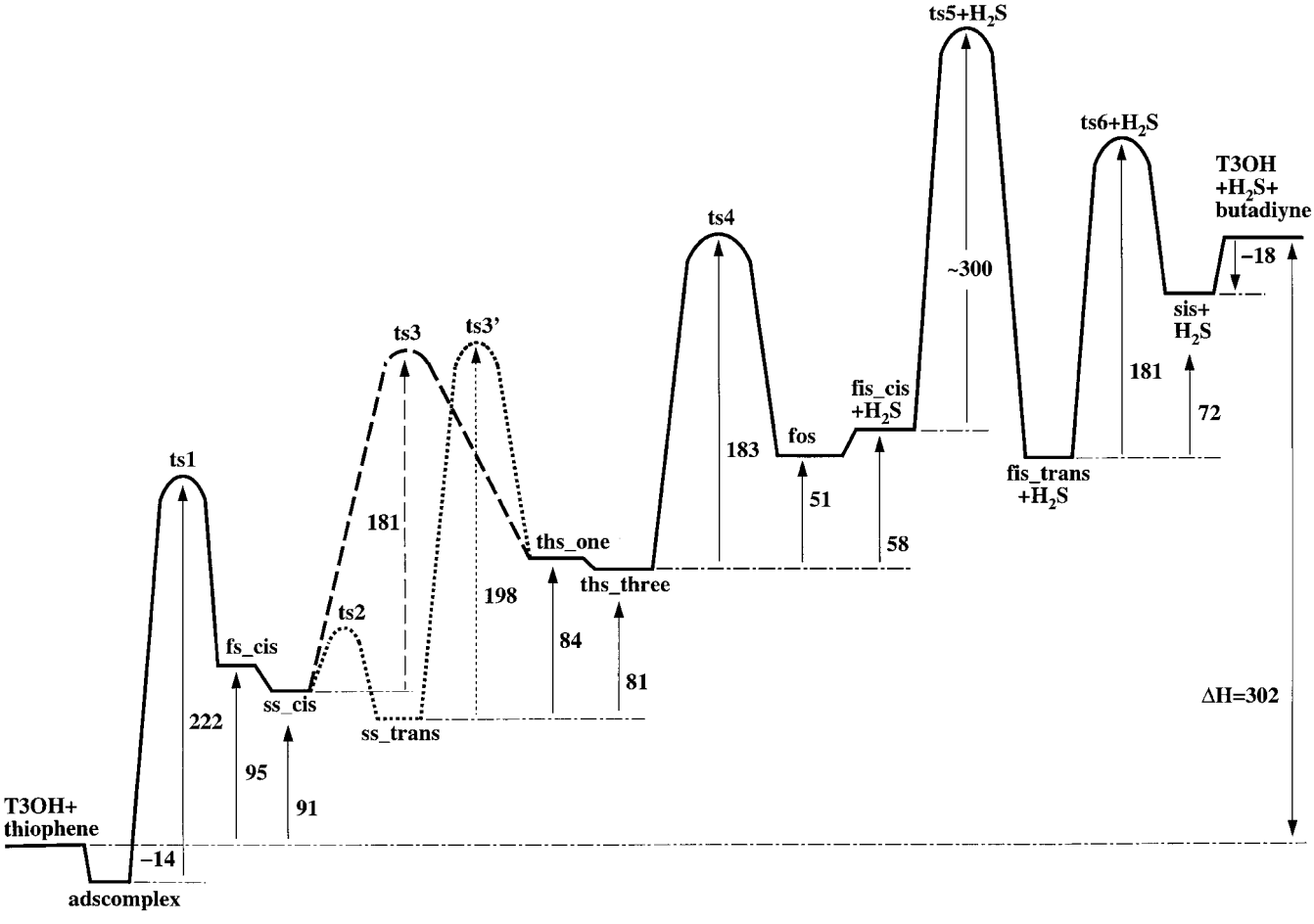

GRAPH 3. The reaction energy diagram of the direct desulfurization in the absence of hydrogen of thiophene catalyzed by a pure acidic zeolite. All the values are in kJ/mol.

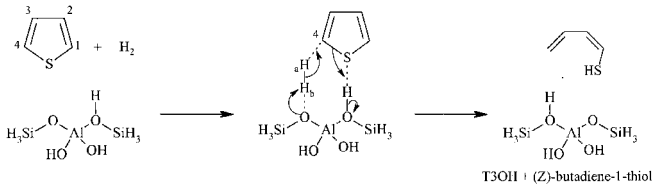

SCHEME 3. A potential concerted mechanism for the opening ring of thiophene in presence of hydrogen.

Desulfurization of Thiophene in the Presence of H_2

Previous results show that in the absence of H_2 desulfurization of thiophene with a pure acidic zeolite is not possible. Hence, the direct influence of H_2 on the reaction mechanism has been studied.

First, one can consider a reaction step where thiophene is adsorbed in the η^1(S) mode and H_2 is adsorbed on an adjacent basic site (Scheme 3). The reaction should then proceed by protonation of the sulfur atom and the S–C4 bond breaking while the Ha–Hb bond breaking occurs leading to the protonation of carbon C4 and back-donation of proton Hb to the cluster. The transition state for such a concerted mechanism could not be obtained. We believe that the size of the "reacting ring" and the weakness of the interactions involved (S—HO–Z and H–H—O–Z in particular) make the transition state too unstable to exist. Therefore, one has to consider a several steps mechanism.

The mechanism of thiophene desulfurization in the presence of H_2 can also be divided into two parts. The first part involves the ring opening of thiophene followed by its hydrogenation leading to the formation of butadiene-1-thiol [*C*]. In the second part compound [*C*] is desulfurized and butadiene [*B*] is then formed. Details of this mechanism are provided in Schemes 4 and 5.

The first two steps of the mechanism are identical to the one proposed for the desulfurization of thiophene in the absence of H_2: thiophene is first adsorbed on the acidic site of the cluster to form the species **ads_complex** and then the thiophenic ring opening occurs leading to compound **fs_cis**. Then, two similar pathways are possible: either compound **fs_cis** can be hydrogenated (Scheme 4, path A) or can swivel through the C2–C3 bond to form structure **fs_trans**, which will then be hydrogenated (Scheme 4, path B). The activation barrier for the *cis–trans* isomerization should be close to +20 kJ/mol as this reaction is nearly the same as to the isomerization of compound **ss_cis** (Scheme 1).

The adsorption complex of H_2 on a basic site of the cluster in compounds **fs_cis** and **fs_trans** could not be computed. All attempts to optimize such a structure led to the desorption of H_2. This is only due to the deficiency of the DFT method that does not describe well the weak van der Waals interactions (8, 9). In the case of hydrogen adsorption the Born repulsive interactions dominate which make the optimization of H_2 adsorption complex impossible. Therefore,

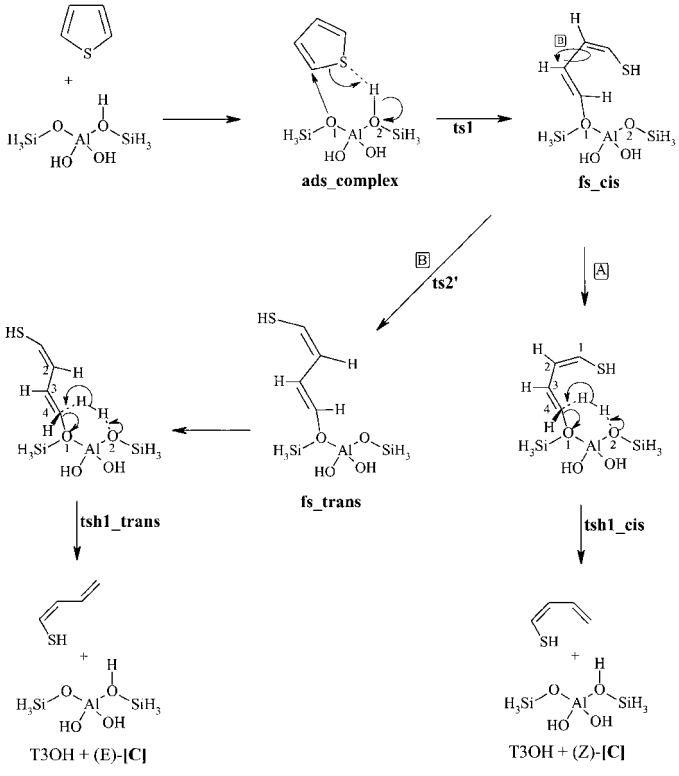

SCHEME 4. The first part of the desulfurization of thiophene by direct desulfurization in the presence of hydrogen reaction pathway mechanisms: opening of the thiophenic ring catalyzed by a pure acidic zeolite.

the activation barrier will be referred to the state where hydrogen does not interact with the cluster. The interaction energy of H_2 with micropore oxygen atoms should be on the order of ~10 kJ/mol or less.

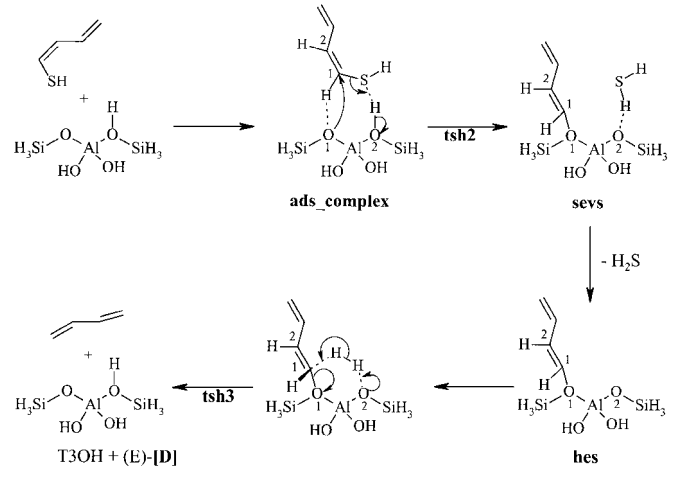

SCHEME 5. The second part of the desulfurization of thiophene by direct desulfurization in the presence of hydrogen reaction pathway mechanisms: removal of the sulfur atom of butadiene-1-thiol catalyzed by a pure acidic zeolite, leading to the formation of butadiene. Here, only the mechanisms involving the *trans* isomer compound are presented.

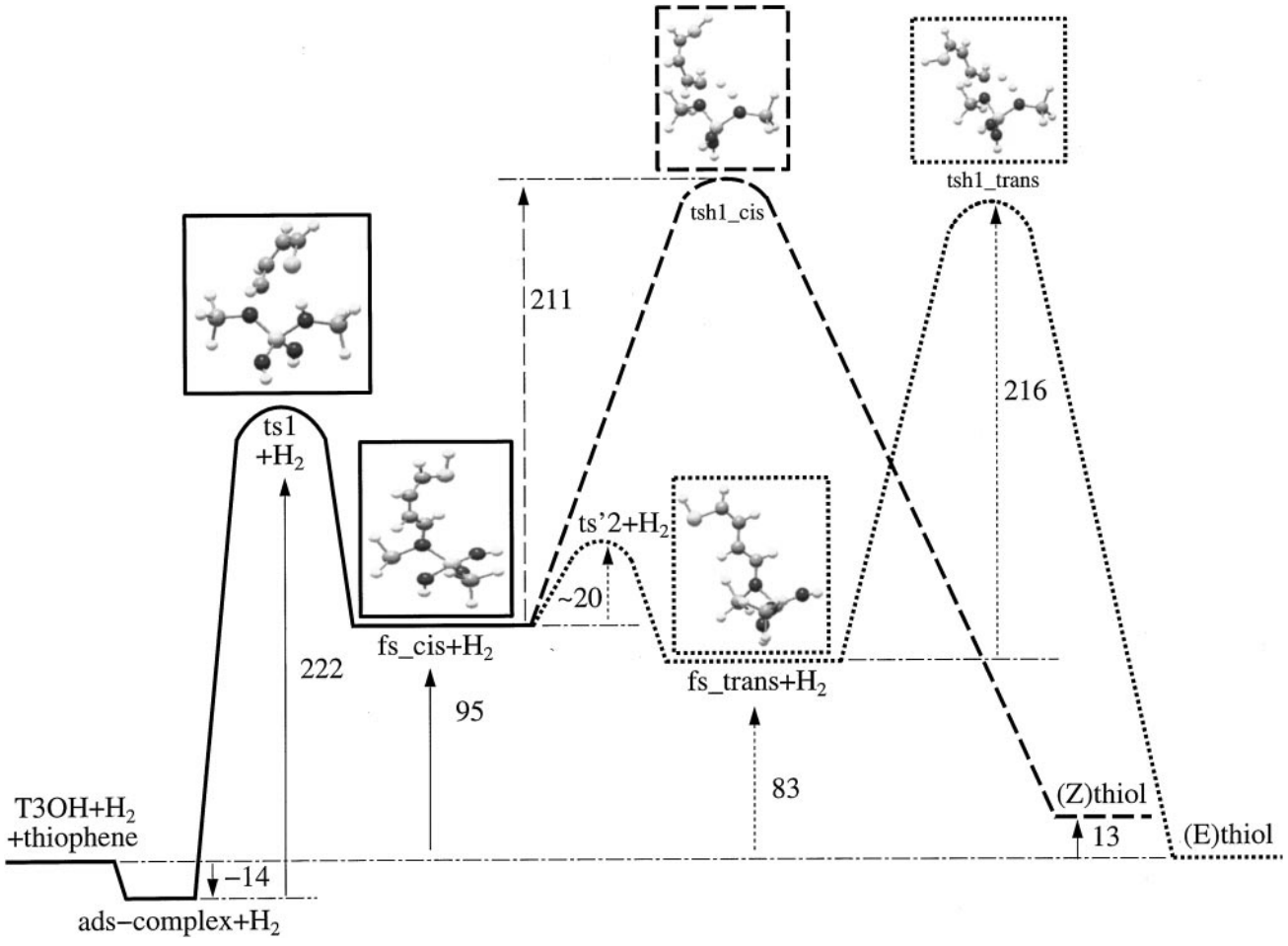

GRAPH 4. The reaction energy diagram and geometries of the transition states and intermediates for the first part of the direct desulfurization in the presence of a hydrogen reaction path of thiophene catalyzed by a pure acidic zeolite. All the values are in kJ/mol.

Hydrogenation of compounds **fs_cis** and **fs_trans** leads, respectively, to (Z)- and (E)-butadiene-1-thiol. Structures of transition states **ts1h_cis** and **ts1h_trans** are very similar as one can see in Graph 4. Moreover, the activation energies are very close (+211 and +216 kJ/mol). Hence, one can conclude that the reaction will occur indiscriminately via path A or path B.

The adsorption complexes of compounds [*C*] in end-on and side-on positions have not been optimized. Indeed, these complexes should be very similar to the ones found for compound [*A*] and from previous results one can conclude that the adsorption energy should be close to −32 kJ/mol.

The second part of the mechanism is basically the desulfurization of compounds [*C*] which leads to the formation of dienes [*D*] (Scheme 5). Two parallel routes can occur simultaneously: one for the *cis* isomer and one for the *trans* isomer. In Scheme 5, only the mechanisms involving the *trans* isomer have been presented.

After adsorption of compounds [*C*] on the zeolite in a side-on position, the proton is transferred to the sulfur atom and C1–S bond breaking occurs. A molecule of H_2S is then formed along with another species covalently bonded to an oxygen. The activation barrier is 167 kJ/mol when the *cis* isomer is involved and 180 kJ/mol with the *trans* isomer. The transition states have similar geometries as one can see in Graph 5.

Next, H_2S desorbs from the cluster leading to structure **hes** (Scheme 5). The structure of compound **sevs** has not been optimized, as we know from the previous mechanism that **sevs** and **hes** have analogous geometries and that desorption of H_2S costs around 7 kJ/mol to the system. Hence, as compounds **hes** lie 32 kJ/mol above diene [*C*], one can conclude that the difference in energy between compounds **sevs** and [*C*] should be around 40 kJ/mol.

After adsorption of H_2 on a basic site of the cluster, protonation of carbon C1 and oxygen O2 occur and finally

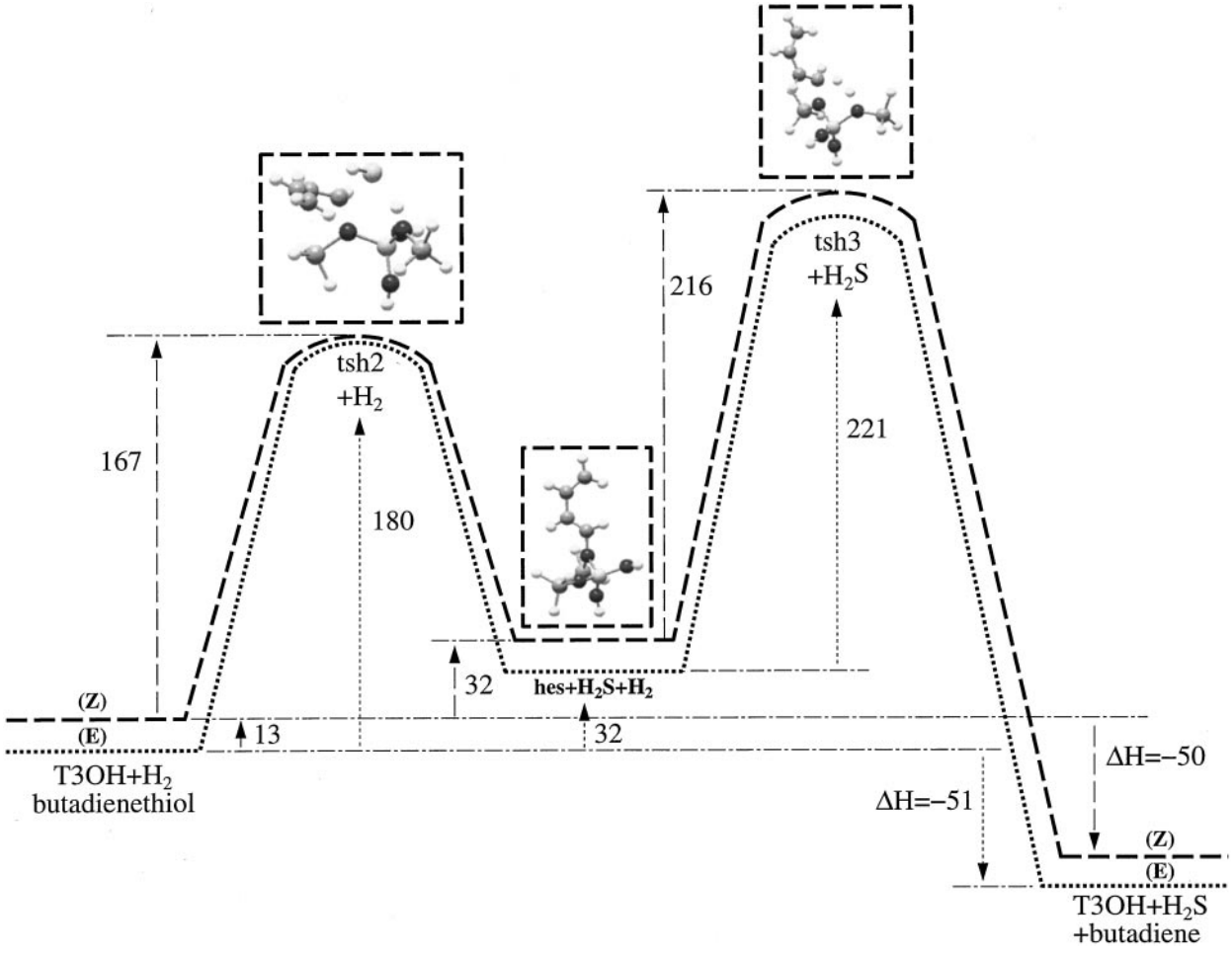

GRAPH 5. The reaction energy diagram and geometries of the transition states and intermediates for the second part of the direct desulfurization in the presence of a hydrogen reaction path of thiophene catalyzed by a pure acidic zeolite. All the values are in kJ/mol.

butadiene is formed. The activation barrier for this step is 216 and 221 kJ/mol, respectively, for **(Z)-hes** and **(E)-hes**.

As one can see in Graph 6, both routes are energetically identical. Small differences in activation barriers exist but are not significant—the main feature being that activation energies for the steps which involves the (Z) isomers are lower than the ones involving the (E) isomers. This may be due to the fact that all (Z) intermediaries are thermodynamically less favored than the (E) species and so will be slightly more reactive. However, reaction will proceed indiscriminately via path A or path B.

When H_2 is present the final product of the desulfurization reaction will not be butadiyne. This will dramatically change the energetic profile of the reaction (Graph 6 and Table 1). Indeed, in the presence of hydrogen the reaction is not anymore endothermic but exothermic with an overall enthalpy of reaction around −40 kJ/mol. This study shows that desulfurization of thiophene, using a nonpromoted acidic zeolite, even when hydrogen is present is a difficult process, but can occur. This conclusion agrees with experimental results (4, 6). Based on the activation energies, one has to conclude that the thiophenic ring opening step is the rate limiting step of the mechanism.

Comparison of the Two Mechanisms

The mechanisms of thiophene desulfurization in the absence and in the presence of hydrogen are very similar. The first part of the reaction cycles corresponds to the ring opening of thiophene and subsequent formation of thiol derivatives. The second part deals with the thiol derivative desulfurization and leads to tetra-carbonated hydrocarbons.

Both mechanisms have high activation energies (∼200 kJ/mol). As mentioned before, the first step of both mechanisms is the same. The second step is either the back-donation of a proton to the cluster (Scheme 1) or the hydrogenation of the species **fs_cis** (Scheme 4). From the values of activation barriers calculated for this step, one can conclude that back-donation of the proton is slightly favored to

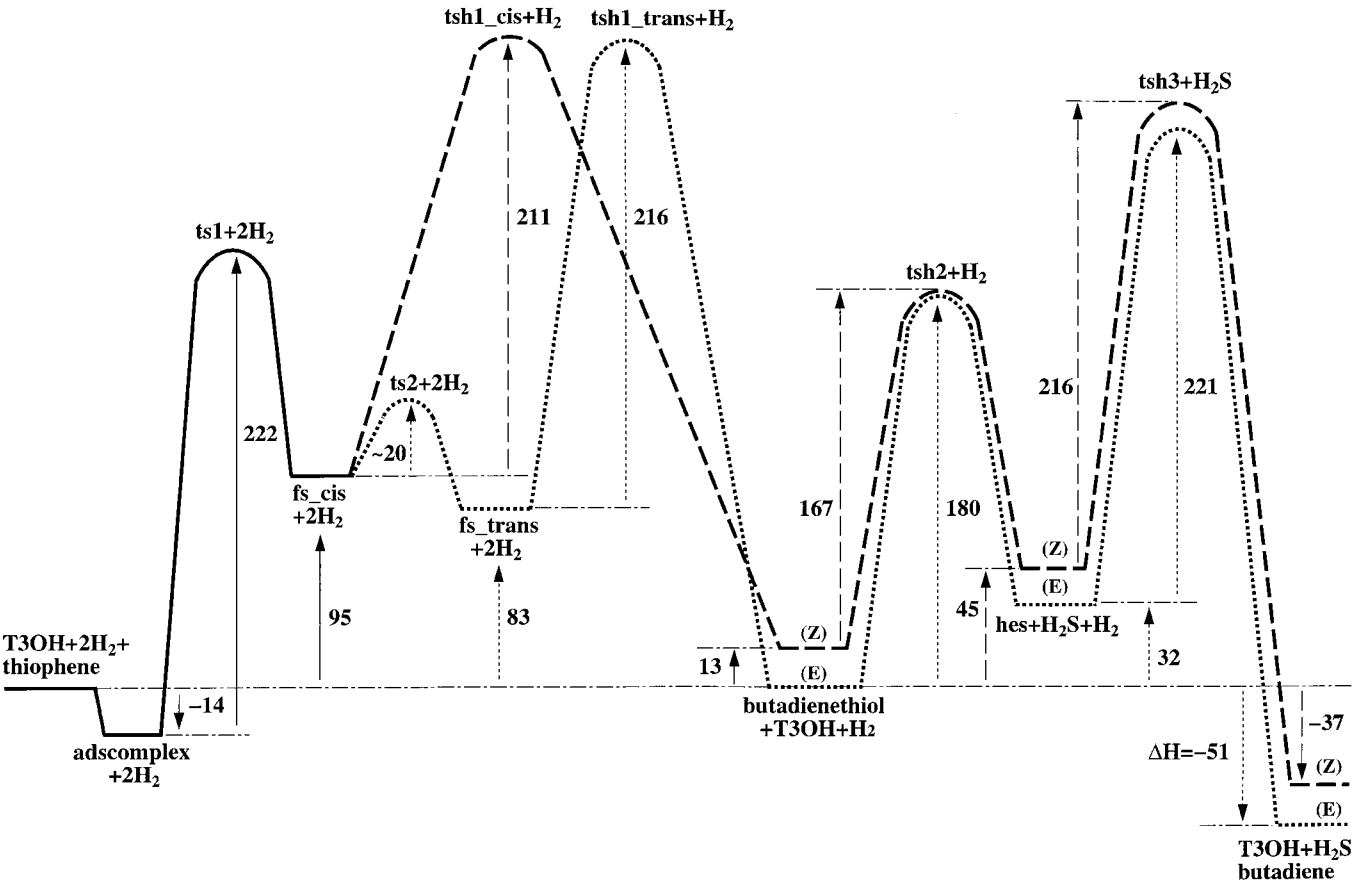

GRAPH 6. The reaction energy diagram of the direct desulfurization in the presence of hydrogen of thiophene catalyzed by a pure acidic zeolite. All the values are in kJ/mol.

hydrogenation (Graphs 3 and 6). However, one must not forget to take into account the enthalpy of reaction. Indeed the back-donation step leads to an enthalpy of reaction around +80 kJ/mol while the one for the hydrogenation step is around −80 kJ/mol. Hence, the step involving the hydrogenation reaction will be the preferred one, from the thermodynamic point of view. The third step of the mechanism is analogous in both mechanisms and consists of a C–S bond cleavage step (Schemes 2 and 5) which involves similar activation barriers. In the second mechanism the *cis–trans* isomerization step does not occur: to perform the next step no hydrogen needs to be near the basic center of the cluster.

As mentioned before, the main difference between those two mechanisms lies in the overall enthalpies of the reactions. Whereas each step of the mechanism in the absence of hydrogen is highly endothermic (Graph 3), the mechanism in the presence of hydrogen leads to a succession of endothermic and exothermic reactions (Graph 6) with a negative overall enthalpy of reaction.

From these results, one can conclude that when using an acidic zeolite as a catalyst hydrogen is mandatory in the desulfurization process.

CONCLUSION

The density functional theory study of zeolite catalyzed desulfurization of thiophene shows that such a reaction can occur only if hydrogen is present. Hydrogen will not decrease activation barriers of the process but will change the intermediates involved and thus will dramatically change the intrinsic thermodynamics of the reactions. Consequently, under catalytic cracking conditions desulfurization of thiophene is possible at severe conditions. But, if hydrogen is present, another reaction pathway can also be considered. The hydrogenation prior to desulfurization of thiophene is possible. The computed activation energy of the thiophenic opening of the ring of dihydrothiophene is lower than the one in the case of the thiophenic opening of the ring of thiophene (+181 kJ/mol). It should be pointed out that there are several possible pathways to consider if hydrogenation reactions happen. The results shown here can be used as a starting point for more calculations involving a zeolite cluster.

Moreover, as a synergy between small metal sulfide particles and the acidic support have been observed with some catalysts (4), it is very likely that in conventional HDS some

steps of the desulfurization mechanism are acid catalyzed, whereas others are metal catalyzed. Hence, knowledge of the energetics of the reaction steps involved when a purely acid catalyst is used is useful in order to understand the reactivity of thiophenic compounds upon contact with bifunctional catalysts.

ACKNOWLEDGMENTS

X. Saintigny thanks Total Raffinage Distribution for sponsorship. Computational resources were partly supplied by the Dutch National Computer Facilities under Project SC-451.

REFERENCES

1. (a) Chianelli, R. R., *Catal. Rev.-Sci. Eng.* **26**, 361 (1984). (b) Prins, R., de Beer, V. H. J., and Somorjai, G. A., *Catal. Rev.-Sci. Eng.* **31**, 1 (1989).
2. Grange, P., and Vanhaeren, X., *Catal. Today* **36**, 375 (1997).
3. (a) Leglise, J., Janin, A., Lavalley, J. C., and Cornet, D., *J. Catal.* **114**, 388 (1988). (b) Cid, R., Fierro, J. L. G., and López Agudo, A., *Zeolites* **10**, 95 (1990). (c) Kovacheva, P., Davidova, N., and Nováková, J., *Zeolites* **11**, 54 (1991). (d) Ezzamarty, A., Catherine, E., Cornet, D., Hemidy, J. F., Janin, A., Lavalley, J. C., and Leglise, J., *Stud. Surf. Sci. Cat.* **49**, 1025 (1989).
4. Welters, W. J. J., de Beer, V. H. J., and van Santen, R. A., *Appl. Catal. A* **119**, 253 (1994).
5. López Agudo, A., Benitez, A., Fierro, J. L. G., Palacios, J. M., Neira, J., and Cid, R., *J. Chem. Soc., Faraday Trans.* **88**, 385 (1992).
6. (a) Blaszkowski, S. R., and van Santen, R. A., *J. Am. Chem. Soc.* **118**, 5152 (1996). (b) Blaszkowski, S. R., Nascimento, M. A. C., and van Santen, R. A., *J. Phys. Chem.* **100**, 3463 (1996).
7. (a) Gale, J. D., *Topics Catal.* **3**, 169 (1996). (b) Boys, S. F., and Bernardi, F., *Mol. Phys.* **19**, 553 (1970).
8. van Santen, R. A., *Catal. Today* **30**, 377 (1997).
9. Sauer, J., Ugliengo, P., Garrone, E., and Saunders, V. R., *Chem. Rev.* **94**, 2095 (1994).
10. van Santen, R. A., *J. Mol. Catal. A* **115**, 405 (1997).
11. Frisch, M. J., Trucks, G. W., Schlegel, H. B., Gill, P. M. W., Johnson, B. G., Robb, M. A., Cheeseman, J. R., Keith, T., Petersson, G. A., Montgomery, J. A., Raghavachari, K., Al-Laham, M. A., Zakrzewski, V. G., Ortiz, J. V., Foresman, J. B., Cioslowski, J., Stefanov, B. B., Nanayakkara, A., Challacombe, M., Peng, C. Y., Ayala, P. Y., Chen, W., Wong, M. W., Andres, J. L., Replogle, E. S., Gomperts, R., Martin, R. L., Fox, D. J., Binkley, J. S., Defrees, D. J., Baker, J., Stewart, J. P., Head-Gordon, M., Gonzalez, C., and Pople, J. A., *in* "Gaussian 94, Revision D.4." Gaussian, Inc., Pittsburgh, 1995.
12. Dunning, T. H., Jr., and Hay, P. J., *in* "Modern Theoretical Chemistry" (H. F. Schaefer, III, Ed.), pp. 1–28. Plenum, New York, 1976.
13. Topsoe, H., Clausen, B. S., and Massoth, F. E., *in* "Hydrotreating Catalysis." Springer-Verlag, Berlin, 1996.
14. (a) Thamm, H., *Zeolites* **7**, 341 (1987). (b) Wu, P., Debebe, A., and Ma, Y. H., *Zeolites* **3**, 118 (1983). (c) Tsikoyiannis, J. G., and Wei, J., *Chem. Eng. Sci.* **46**, 233 (1991).
15. Calderbank, K. E., Calvert, R. L., Lukins, P. B., and Ritchie, G. L. D., *Aust. J. Chem.* **34**, 1835 (1981).
16. "Handbook of Chemistry and Physics," 71st ed. CRC Press, Boca Raton, 1990.
17. March, J., *in* "Advanced Organic Chemistry: Reactions, Mechanisms, and Structures," 4th ed., p. 129. Wiley-Interscience, NewYork, 1992.